Research Article

Somdutt Mujwar#, Jyoti Pal#, Manu Sharma*, Abhishek Tiwari, Varsha Tiwari, Manish Kumar, Shivani Verma, Ashraf Ahmed Qurtam, Fahd A. Nasr, Mohammed Al-Zharani, Abdulsalam Alhalmi

Computational design and *in vitro* assay of lantadene-based novel inhibitors of NS3 protease of dengue virus

https://doi.org/10.1515/chem-2024-0004
received December 22, 2023; accepted February 19, 2024

Abstract: Dengue virus (DENV) infection is one of the diseases for which no drug is available for the treatment. The DENV NS2B-NS3 protease is considered to be the prime target for anti-dengue drug development because of its importance in the development of new virus subunits via DENV poly-protein breakdown. Pentacyclic triterpenoids (Lantadenes) from the weed *Lantana camara* L. and its semi-synthetic congeners have shown a wide array of biological activities in the last two decades. The virtual screening strategy was used on the library of 78 natural and semi-synthetic lantadenes to predict the potent antagonists for the NS2B-NS3 protease enzyme of DENV and their experimental validation by *in vitro* assay of lead molecules. In the *in silico* analysis of 78 triterpenoids, two lead molecules (−10.60 and −9.93 kcal/mol) were predicted to be inhibitors of protease (viral) when compared to its reference ligand 1,8-dihydroxy-4,5-dinitroanthraquinone (−5.377 kcal/mol). At the same time, binding affinity, pharmacokinetic, and toxicity profiling, along with molecular dynamics simulations, were studied. The *in vitro* viral infection inhibition assay inferred that lead molecule **62** exhibited a 60% and 45% reduction in DENV titers at 10 and 5 μM concentrations, respectively. The lead molecule **62** can further be optimized for its pharmacophore and has the potential to be developed as a drug-like molecule.

Keywords: lantadenes, dengue virus, NS2B-NS3 protease, *in silico* analysis

1 Introduction

Dengue virus (DENV) is a pathogenic parasitic organism belonging to the disease-causing family of Flaviviruses. The viral genome of DENV is a single-stranded RNA having about 11k nucleotides encoding three major structural proteins of the viral capsid, envelop protein, membrane proteins, as well as seven non-structural proteins, i.e., NS1, NS2A, NS2B, NS3, NS4A, NS4B, and NS,5 which are majorly involved in the biochemical processes of the viral pathogen [1]. The viral genome of DENV encodes for a single polyprotein that further undergoes fragmentation at the surface of the host's rough ER by the viral NS2B/NS3 protease enzyme. DENV protease enzyme is a serine protease belonging to the chymotrypsin enzyme family having a catalytic triad in

# Equal contribution.

*** Corresponding author: Manu Sharma,** Department of Chemistry and Toxicology, National Forensic Sciences University, Delhi Campus, New Delhi 110085, India, e-mail: lantadene@hotmail.com
Somdutt Mujwar: Chitkara College of Pharmacy, Chitkara University, Rajpura 140401, India; Centre of Excellence, Drug Design and Molecular Modelling Centre, Chitkara College of Pharmacy, Chitkara University, Rajpura-140401 Punjab, India, e-mail: somduttmujwar@gmail.com
Jyoti Pal: Department of Chemistry and Toxicology, National Forensic Sciences University, Delhi Campus, New Delhi 110085, India, e-mail: jyotipalmha@gmail.com
Abhishek Tiwari: Pharmacy Academy, IFTM University, Lodhipur-Rajput, Moradabad, India, e-mail: abhishekt1983@gmail.com
Varsha Tiwari: Pharmacy Academy, IFTM University, Lodhipur-Rajput, Moradabad, India, e-mail: varshat1983@gmail.com
Manish Kumar: Department of Pharmaceutics, ISF College of Pharmacy, Moga, Punjab, India, e-mail: manish_singh17@rediffmail.com
Shivani Verma: School of Pharmacy, Graphic Era Hill University, Dehradun 248002 India, e-mail: shivaniverma@gehu.ac.in
Ashraf Ahmed Qurtam: Department of Biology, College of Science, Imam Mohammad Ibn Saud Islamic University (IMSIU), Riyadh 11623, Saudi Arabia, e-mail: aaqurtam@imamu.edu.sa
Fahd A. Nasr: Department of Biology, College of Science, Imam Mohammad Ibn Saud Islamic University (IMSIU), Riyadh 11623, Saudi Arabia, e-mail: faamohammed@imamu.edu.sa
Mohammed Al-Zharani: Department of Biology, College of Science, Imam Mohammad Ibn Saud Islamic University (IMSIU), Riyadh 11623, Saudi Arabia, e-mail: mmyalzahrani@imamu.edu.sa
Abdulsalam Alhalmi: Department of Pharmaceutics, School of Pharmaceutical Education and Research, Jamia Hamdard, New Delhi 110062, India, e-mail: asalamahmed5@gmail.com

the form of Ser-His-Asp [2]. The biochemical functioning of the viral NS3 protease enzyme is regulated via an NS2B cofactor for recognition of the substrate. Eight out of the 13 polyprotein cleavage sites are cleaved by the viral protease for further processing and maturation into the viral particles, making it an appropriate target for developing novel drugs for the treatment of dengue [3].

Natural products offer a wide and complex array of structure and have been responsible for various types of biological activities. Triterpenoids are a class of secondary metabolite plants that have demonstrated different pharmacological properties, including anticancer, antibacterial, antifungal, and anti-viral activities due to their complex and unique structural feature. Triterpenoids from the weed *Lantana camara* L. called Lantadenes (Figure 1) have attracted a lot of interest in the last two decades, and more than a hundred semi-synthetic congeners have been synthesized by us and have been evaluated for their anticancer activities [4–12]. These diverse libraries of compounds have been screened computationally and lead molecules have been studied for their *in vitro* dengue inhibition potential.

2 Materials and methods

2.1 *In silico* analysis

2.1.1 Design of the ligand library

A ligand library of lantadene analogues was prepared using a bioisosteric replacement strategy with the intent to increase its affinity for its macromolecular target and increase its permeability across the plasma membrane to optimize pharmacokinetics for increased bioavailability. Initially the 2D structures of all the concerned ligands were prepared by using the ChemDraw-15.0 tool, followed by converting each of the ligands to stabilized conformation having minimum structural energy with optimized spatial geometry by applying MM2 forcefield of Chem3D software [13]. Optimized 3D structure of each ligand was finally saved in protein databank (*.pdb) format as per compatibility with the AutoDock tool.

2.1.2 Selection and preparation of target proteins

The structural protein model of the viral NS3 protease enzyme was selected on the basis of the lowest resolution of X-ray used for the structural determination via the XRD technique for the refined structural model as well as the presence of a complex ligand for the validation of docking protocol. Structural prototype of the NS3 protease enzyme of DENV co-crystallized with coenzyme NS2B was downloaded from the protein databank (PDB code-2FOM) [14–16]. The bound peptidyl coenzyme-based ligand was detached from the macromolecular complex by using the Chimera tool to obtain nascent receptor and ligand molecules required for docking analysis [17–19]. Macromolecular target was set for docking analysis by removing non-redundant water molecules and assigning Gasteiger charge and addition of polar hydrogens.

2.1.3 Binding site identification

The macromolecular active site was explored by using the DoGSiteScorer module of the Protein Plus webserver by observing the conformational and surface of the target protein. DoGSiteScorer is a grid-based approach that uses Gaussian filters for the identification of pockets and subpockets present in the macromolecular structure. The identified macromolecular active site of the viral NS3 protease enzyme was further utilized for finalizing the grid parameters required for performing docking analysis [20–22].

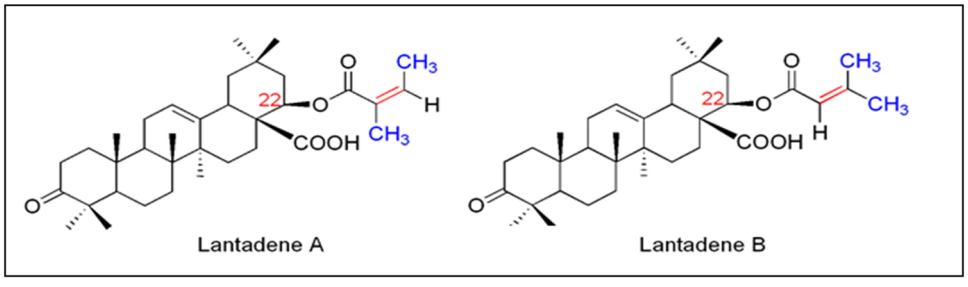

Figure 1: Chemical structures of lantadenes A and B.

2.1.4 Molecular docking

The grid-box prepared by using the prior identified parameters covering the ligand's extended conformations as well as the active residues incorporated in the ligand binding were later utilized for generating map files for specific atoms with the Autogrid software [23–28].

For docking investigations, AutoDock 4.2 software was utilized, which uses the Lamarckian genetic (LG) algorithm for conformational search. The binding energy of each ligand is calculated from a docked atom configuration by utilizing a force field with linear weights as a scoring function. The forcefield estimates the ligand's free binding energy based on the integration by comparative energetics of intramolecular energies for the bound and unbound states of the reference ligand by using a thermodynamic model. The optimized parameters for the docking of the reference crystallized ligand were saved in the docking parameter file and are utilized for the docking analysis of newer ligands [29–31].

2.1.5 *In silico* screening

The molecular ligand library of 78 lantadene-based ligand molecules was further utilized to execute computational screening against the viral NS3 protease enzyme to predict the potent leads based on their binding affinities (Table S1, supplementary information). The interacting macromolecular residues actively involved in the binding of the concerned ligands were specifically analyzed to predict the affinity of the specific ligand against the viral NS3 protease enzyme. The utilized docking parameters were further evaluated to validate that the executed method based on the resulting binding energy for the reference ligand should fall well within the defined range. The validated parameters were further employed for the docking analysis of the ligands of the prepared library, and the leads were shortlisted for further analysis based on their highest affinity and lowest binding energy against the concerned antiviral target. Lamarckian Genetic algorithm was the scoring function of the AutoDock tool to evaluate their binding affinity for the target receptor [32–38].

2.1.6 Pharmacokinetic and toxicological profiling

The lead molecules need to have discrete physicochemical properties that facilitate the smooth movement of the drug within the human body to impart long-lasting and potent therapeutic effects. The pharmacokinetics optimization by absorption, distribution, metabolism, and excretion (ADME) is a crucial step in developing a new drug molecule. It has been observed that the physicochemical properties of the small chemical moieties play a significant role in controlling their ADME, and their pharmacokinetics can be optimized by making small structural changes. Nowadays, computational modeling is a trending approach for optimizing the pharmacokinetic profile of a small molecule and is considered as highly reliable for predetermining the pharmacokinetic behavior of a newer lead drug development regimen. These computational modeling approaches for pharmacokinetic modeling were proven to be an economical and faster alternative to the experimental methods [39–41]. pkCSM webserver was utilized in this study to evaluate critical drug-like characteristics based on the physicochemical and pharmacological features of shortlisted leads based on Lipinski's rule of five.

2.1.7 Molecular dynamic simulation

Based on the observed docking outcome and their safety profile, lead compound **62** was shortlisted post-computational screening for proceeding further to analyze its thermodynamic stability by executing MD simulation. The nominated lead molecule was first exposed to a simulation for a timeframe of 100 ns to confirm the complex stability with regard to time at a fixed temperature of 300 K. Desmond software by Schrodinger was utilized to simulate the dynamic nature of ligand **62** complexed within the macromolecular target. The ligand–receptor complex was solvated in an explicit water box by employing an OPLS3e force field. The preferred SPC (single point charge) model was inferred for the explicit water molecules by using the OPLS3e force field for the simulation of macromolecular complexes having small ligands for the best repeatable results [42–45].

The displacement of the residues of the macromolecular receptor and the ligand from their original positions within a specific time period during their binding process was determined using their root mean square deviation (RMSD). The movement of the macromolecular residues from their initial positions in the structural model was calculated as the root mean square fluctuation (RMSF). The structural arrangements of the macromolecular secondary structure elements (SSE), such as α-helices and β-strands, were calculated by considering their consistent residue index during simulation. The chemical interactions existing between the macromolecular target and the bound ligand during the simulation were assessed by hydrogen bonds, hydrophobic interactions, ionic bonds, and interactions

via the formation of water bridges. The ligand's RMSD value was determined by its relative movement with reference to its initial frame during the simulation. The ligand's extended length, corresponding to its primary moment of inertia, was determined using rGyr MolSA, which represents van der Waal's surface area. The contribution of oxygen and nitrogen atoms was considered in estimating the polar surface area (PSA), while rGyr MolSA was calculated using a 1.4 probe radius.

2.2 Methodology for the synthesis of lead compounds

2.2.1 General experimental procedures

The procedure and conditions of synthesis are described in Supplementary information. All the reagents and solvents were purchased from local Indian suppliers (Ranchem, S D Fine) and were used without further purification or distillation unless otherwise stated.

2.2.2 Plant material, extraction, and isolation of lantadenes

Lantana camara L. leaves were collected in July 2022 from Palampur, Himachal Pradesh, India. The plant was authenticated by a qualified botanist and taxonomist, and herbarium sheet (LCL/2022/234) was submitted. The leaves were dried and powdered. Lantadenes A and B were isolated in their pure form, as described in our previous publications, and the purity of Lantadenes A and B was ascertained by spectroscopic studies [4].

2.2.3 Synthesis of lead molecules (62 and 64)

The synthesis was carried out by the procedure as reported by us previously [5–8]. The detailed scheme and spectral data are provided as supplementary information.

2.2.4 *In vitro* dengue inhibition assay

The lead molecules identified after computational screening were synthesized and screened for their antiviral activities on A549 cell lines. The cells (~50,000) were seeded in a 48-well plate and infected with the DENV2 strain at five MOI for 1 h. The infected cultures were incubated for 1 h in the culture media with selected lead molecules at two different concentrations (10 or 5 µM). After 24 h post-infection, viral titers in the supernatants were estimated by a plaque assay, as published previously [46].

3 Results

3.1 Ligand designing

With the intent to increase the affinity against the concerned receptor as well as to optimize the pharmacokinetics of the resulting compound, bioisosteric substitutions have been executed at C-3 and C-22 of the lantadene nucleus. Based on the executed substitutions, a ligand library of 78 energy-minimized lantadene analogues was prepared by using ChemDraw and Chem3D software.

3.2 Macromolecular target selection

The structural model of the NS3 protease enzyme of DENV procured from the PDB database was resolved by XRD at a resolution of 1.50 Å and an *Escherichia coli*-based expression system. The macromolecular structure of the antiviral drug target has two polypeptide chains: a small polypeptide chain A of the NS2B domain having **62** amino acids and a chain B of the NS3 protease enzyme having 185 amino acids. Chain B of the viral NS3 protease enzyme was used for docking studies by removing the coenzyme structure.

3.3 Molecular docking simulation

The macromolecular target for the current docking protocol was set for docking analysis by adding polar hydrogen atoms, providing equal distribution of Gasteiger charge, and assigning autodock4 atom type to all the macromolecular residues. The grid box was equipped by casing the extended conformations of the reference ligand and interacting residues with the complex ligand. The grid dimensions considered for the current study were x = −5.387, y = −12.72, and z = 13.414, having a size of 40 × 40 × 40 and a spacing of 0.586 Å. The docked reference ligand has identical interactions and is clearly shrouded over biologically active conformation, leading to successful validation of the current docking protocol by chemical resemblance and overlay methods. These validated parameters were further used for performing *in silico* screening of the prepared ligand library against the viral enzyme.

Table 1: Binding energies of the shortlisted lantadene-based leads against the viral NS3 protease enzyme

S. No.	Name/code	Structure	NS3 protease enzyme (PDB id: 2FOM)
1	11	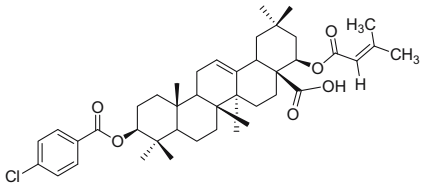	−9.27
2	18	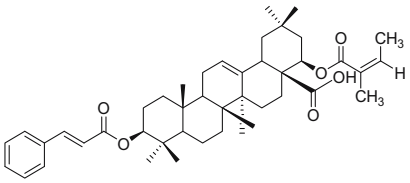	−9.24
3	25	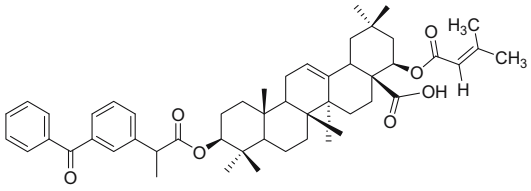	−9.48
4	30	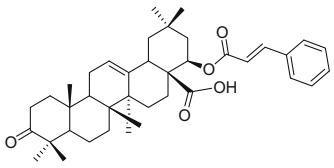	−9.29
5	37	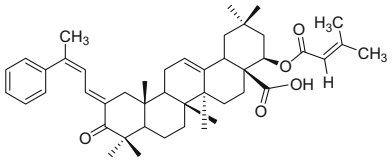	−9.24
6	62	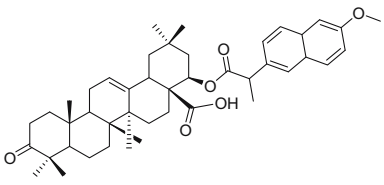	−10.60
7	64	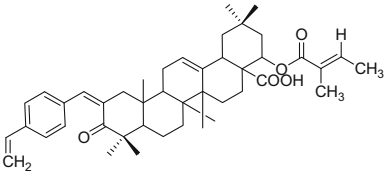	−9.93
8	65	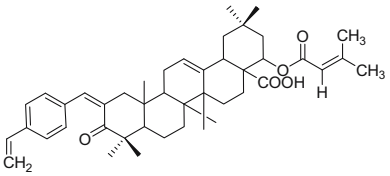	−9.85
9	Reference	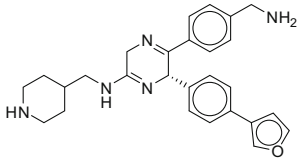	−5.84 (i16)

3.4 *In silico* screening

The docking-based computational screening of a designed molecular library comprising 78 lantadene analogues against the viral NS3 protease enzyme was performed to identify potential leads. The validated grid parameters were used for the virtual screening of the ligand library against the active binding site of the target viral receptor. The obtained docking results are tabulated in Table 1.

3.5 Pharmacokinetic and toxicological profiling

Pharmacokinetic factors control how drugs travel through the human body. The physicochemical, ADME, and toxicity characteristics of the lead compounds were predicted using pkCSM webserver. Table 2 lists the proposed lead's pharmacokinetics and toxicity characteristics. According to Lipinski's rule of five, all of the studied parameters (MW, HBA, HBD,

Table 2: Physicochemical, pharmacokinetics, and pharmacodynamics properties of the selected lead compounds for the viral NS3 protease enzyme

Property	Descriptor	11	18	25	30	37	62	64	65	Reference
MW	(g/mol)	693.365	684.958	791.082	600.84	680.97	684.958	666.943	666.943	441.579
LogP	—	10.2396	9.9858	11.3071	8.6769	10.5695	9.4283	10.2662	10.2662	3.937
Rotatable bond	—	5	6	8	4	5	5	5	5	6
HBA	—	5	5	6	4	4	5	4	4	6
HBD	—	1	1	1	1	1	1	1	1	3
TPSA	$(Å)^2$	297.97	299.707	345.98	263.458	300.269	299.449	293.904	293.904	194.573
Absorption	Water solubility (mol/L)	−3.763	−3.708	−3.333	−3.753	−3.651	−3.705	−3.799	−3.726	−3.647
	$CaCo_2$ permeability	0.75	0.711	0.575	0.685	0.706	0.861	0.809	0.758	0.888
	Intestinal absorption (%) (human)	95.559	98.072	100	98.289	99.122	99.958	99.719	99.286	92.131
	Skin Permeability (Log Kp)	−2.735	−2.735	−2.735	−2.735	−2.735	−2.735	−2.735	−2.735	−2.778
	P-glycoprotein substrate	No	Yes	Yes	Yes	Yes	No	Yes	Yes	Yes
	P-glycoprotein I inhibitor	No	No	No	No	No	No	No	No	Yes
	P-glycoprotein II inhibitor	Yes	Yes	No	Yes	Yes	Yes	Yes	Yes	Yes
Distribution	VDss (human)	−0.805	−0.979	−1.153	−0.784	−1.187	−0.676	−1.096	−1.129	1.822
	Fraction unbound (human)	0	0	0.037	0	0	0	0	0	0.131
	BBB permeability	−0.603	−0.426	−0.686	−0.185	−0.106	−0.328	−0.12	−0.122	−0.376
	CNS permeability	−1.755	−1.787	−1.756	−0.994	−0.624	−1.889	−0.695	−0.704	−2.029
Metabolism	CYP2D6 substrate	No	No	No	No	No	No	No	No	No
	CYP3A4 substrate	Yes	Yes	Yes	Yes	Yes	Yes	Yes	Yes	Yes
	CYP1A2 inhibitor	No	No	No	No	No	No	No	No	Yes
	CYP2C19 inhibitor	No	No	No	No	No	No	No	No	No
	CYP2C9 inhibitor	No	No	No	No	No	No	No	No	No
	CYP2D6 inhibitor	No	No	No	No	No	No	No	No	Yes
	CYP3A4 inhibitor	No	No	No	No	No	No	No	No	Yes
Excretion	Total clearance (log ml/min/kg)	−0.749	−0.405	−0.888	−0.374	−0.618	−0.615	−0.55	−0.636	0.6
	Renal OCT2 substrate	No	No	No	No	No	No	No	No	No
Toxicity	AMES toxicity	No	No	No	No	No	No	No	No	No
	Max. tolerated dose (human) (log mg/kg/day)	0.74	0.6	0.208	0.534	0.574	0.996	0.66	0.62	0.095
	hERG I inhibitor	No	No	No	No	No	No	No	No	No
	hERG II inhibitor	No	No	No	No	No	No	No	No	Yes
	Oral rat acute toxicity (LD50) (mol/kg)	2.774	2.684	2.617	2.662	2.681	2.877	2.732	2.726	2.744
	Oral rat chronic toxicity (LOAEL) (mg/kg/day)	0.402	0.755	0.661	0.977	0.206	1.309	0.268	0.249	1.027
	Hepatotoxicity	No	No	No	No	No	No	No	No	Yes
	Skin sensitization	No	No	No	No	No	No	No	No	No
	T. pyriformis toxicity (mg/L)	0.285	0.285	0.285	0.285	0.285	0.285	0.285	0.285	0.416
	Minnow toxicity	−3.594	−3.664	−5.087	−2.384	−3.222	−1.751	−3.139	−3.055	2.099

TPSA, and LogP) of the selected compounds fall within the optimal range. Compound **62** has been recommended with better pharmacokinetic qualities based on the specified physicochemical parameters. *P*-glycoprotein does not exhibit itself as a substrate for the ligand molecule **62**, serving as a physiological barrier for drugs, toxins, and xenobiotics. For most of the cytochrome P450 isoenzymes, except CYP3A4, compound **62** has not shown substrate-like characteristics. The ligand consistently shows a high propensity to be eliminated from the body via a small number of toxicity pathways, such as hERG-I blocking, sensitization of the skin, toxic effects of *Tetrahymena pyriformis*, hepatotoxicity, and minnow toxicity. The estimated ADME and toxicological parameters of compound **62**, which are based on physicochemical factors, match well within the permitted range, making it a better option for therapeutic development.

3.6 Molecular dynamics simulation

By running a 100 ns MD simulation using the Schrodinger Desmond program, the macromolecular complex of the NS3 protease with the proposed lantadene-based antagonist compound **62** has been further confirmed for its thermodynamic stability. The macromolecular receptor consists of 150 amino acids, and the ligand contains 50 heavy atoms of 110 atoms in total, along with 7 rotatable bonds. RMSD analysis ensures effective implementation of the simulation procedure for validating the structural integrity during the entire operation. Through the alignment of their heavy metals, the ligand's RMSD measurement indicates its stability in relation to the active residues of the target enzyme throughout the simulation. RMSD for the macromolecular residues demonstrated consistent vibrations within the range of 1.2–2.0 Å, indicating that the majority of the residues remained unchanged in their initial positions during the complexation of the ligand molecule. Throughout the simulation run, the RMSD value of the ligand molecule remained stable within the range of 4.8–6.4 Å, without significant deviations. Both the backbone of the macromolecule and the ligand based on lantadene exhibited high stability during the simulation, with minimal fluctuations. The RMSD plot in Figure 2 illustrates the macromolecule and ligand's stability throughout the 100 ns simulation process. RMSF for most of the

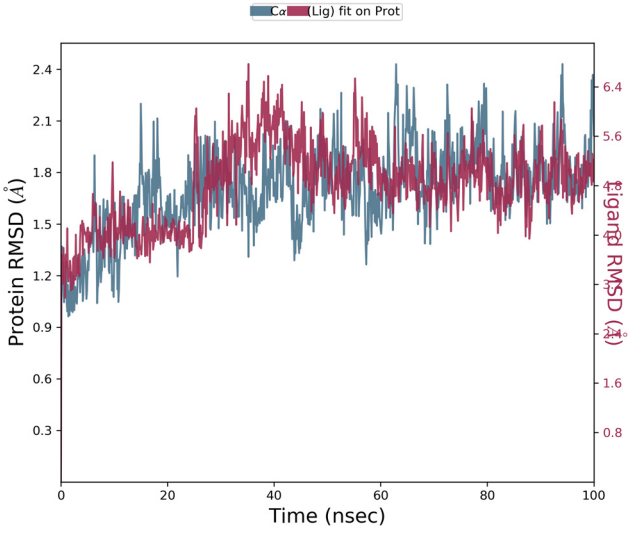

Figure 2: RMSD of the Cα backbones of the viral NS3 protease enzyme and compound **62** observed via MD simulation analysis.

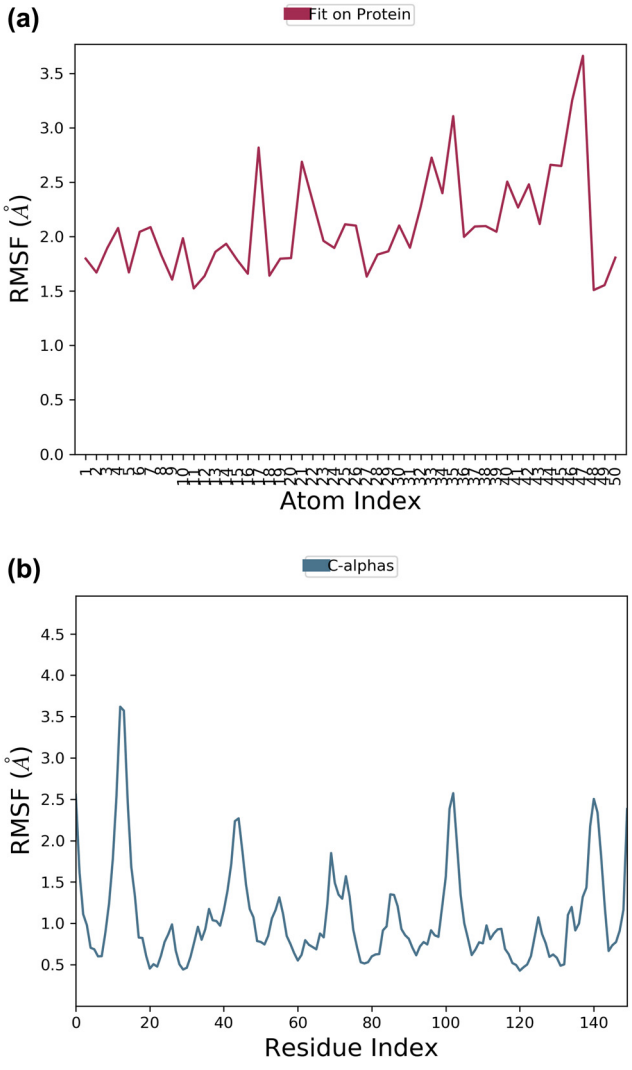

Figure 3: RMSF of the bound lantadene-based compound **62** (a) and the Cα backbone of the viral NS3 protease enzyme (b) observed via MD simulation analysis.

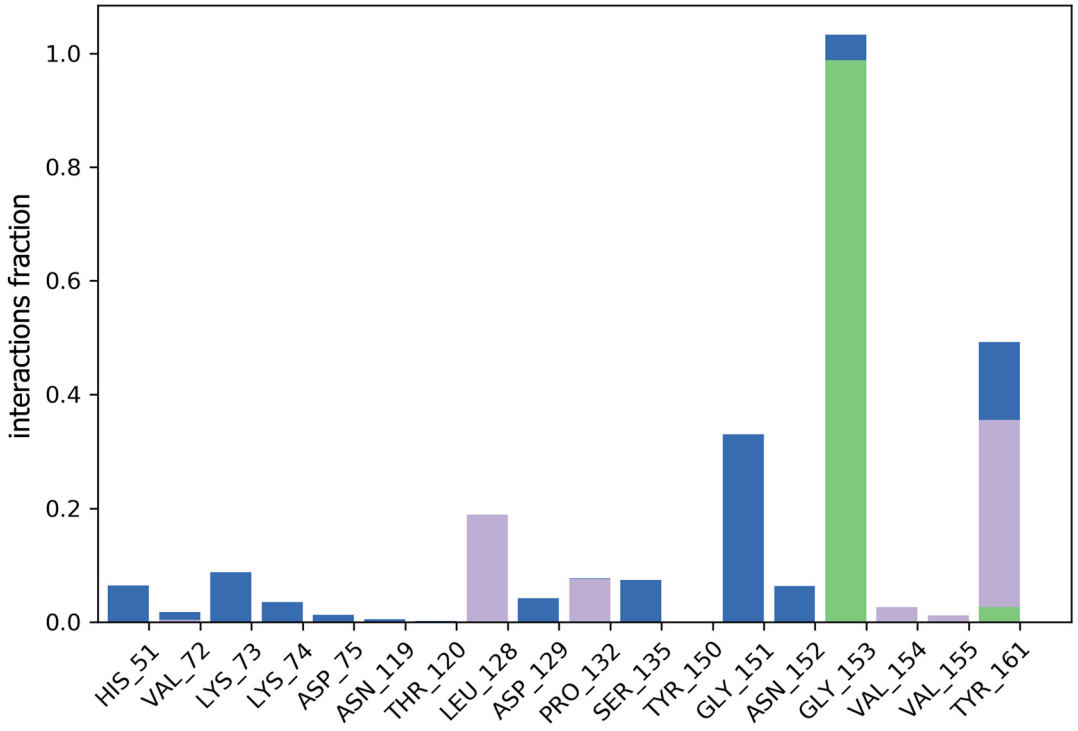

Figure 4: Interactions observed between compound **62** and the macromolecular target during the MD simulation analysis. Water bridges are depicted in blue, H-bonds are depicted in green, and hydrophobic interactions are shown in magenta.

macromolecular amino acids, except some terminal residues, lies within the range of 0.5–2.0 Å, which was well within the allowed range of 3 Å. Figure 3(a) and (b) displays the RMSF of the NS3 protease enzyme and lantadene-based ligand (Compound **62**) during the simulation. RMSF analysis was performed on the ligand complexed within the active site of the target NS3 protease. It was observed that the RMSF values ranged from 2 to 3 Å during the entire 100 ns simulation. This indicates the ligand's stability within the macromolecular active site with only minor alterations in a few functional groups that are essential for interacting with the target macromolecule.

Throughout the simulation, the SSE analysis showed that approximately 2% of the structure consisted of α helices, while about 43% consisted of β strands, resulting in a combined contribution of 45% from SSE, which remained relatively consistent for most of the simulation duration. The investigation of the interactions between the macromolecule and the ligand revealed specific residues, including His51, Lys73, Leu128, Pro132, Ser135, Gly151, Asn152, Gly153, and Tyr161, that interacted with the ligand during the entire 100 ns simulation. A detailed representation of the protein–ligand connections observed during the entire simulation period is shown in Figure 4. Additionally, Figure 5 illustrates the two-dimensional binding interaction between the viral NS3 protease enzyme and the designed lantadene-based inhibitor compound **62**.

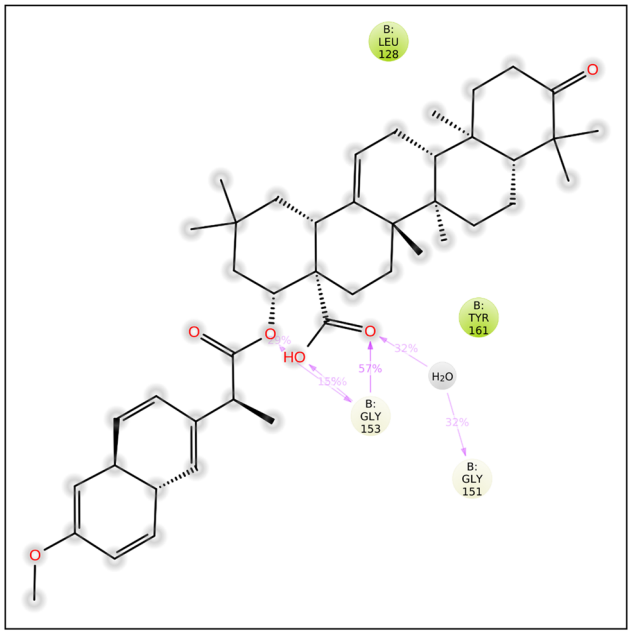

Figure 5: Two-dimensional ligand interactions of compound **62** with the viral NS3 protease enzyme.

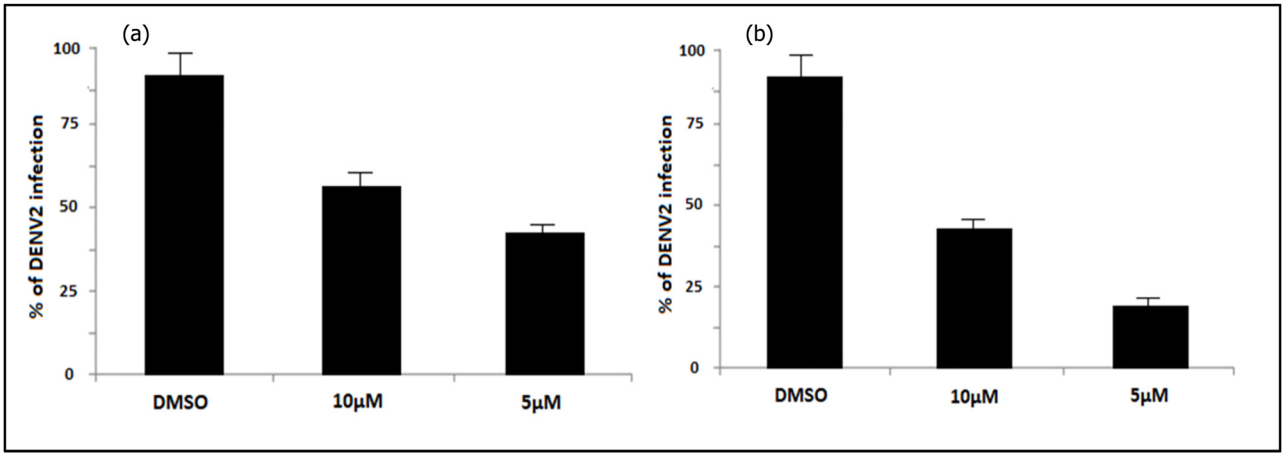

Figure 6: DENV2 strain inhibition by (a) compound **62** and (b) compound **64** at 10 and 5 μM. The 95% confidence intervals of geometric means were used for error bars.

3.7 *In vitro* dengue inhibition activity

The two lead molecules **(62, 64)** were identified by computational screening of 78 lantadene congeners. The lead molecules were screened for inhibitory assay of dengue *in vitro*. The results showed that compound **62** reduced DENV titers by 60% and 45% at 10 and 5 μM concentrations, respectively (Figure 6a). However, compound **64** exhibited a 40% and 15% reduction in the DENV titers at 10 and 5 μM concentrations, respectively (Figure 6b). Compound **62** has been previously developed by us as NF kappa B inhibitors in various cancer cell lines. In docking studies against the viral NF kappa B receptor, compound **62** showed maximum efficacy. The results indicate that compound **62** can be a promising candidate for the development of DENV infection. Further, optimization of the pharmacophore and ADME studies are vital to developing lead molecule **62** as a promising NCE against DENV.

4 Discussion

Computational designing methods, including docking and dynamic simulation, are highly reliable approaches to predicting the molecular behavior of ligands within the macromolecular cavity. The predicted molecular behavior of the newer ligands based on the chemical laws helps determine the binding affinity toward the specific target receptor. The computational techniques are very fast, economical, and multitasking in nature, which fastens the drug discovery process with reduced economic burden and a higher rate of success [47].

Lantadenes are a group of compounds having pentacyclic triterpenoid oleanane nucleus, which was first obtained from the plant *Lantana camara* and exhibited diverse therapeutic potential including anticancer, antimicrobial, anti-inflammatory, antimalarial, antiulcer, insecticidal, antihyperglycaemic, antihypertensive, anti-urolithiatic, and wound healing [48]. Reported for multiple therapeutic potentials of lantadene derivatives, a series of lantadene analogues were designed by considering diverse functionalities based on the bioisosteric replacements to evaluate their therapeutic potential against DENV. The NS3 protease enzyme is a vital component of the DENV involved in the vital process of replication and processing of viral polyproteins required for the execution of the viral life cycle and causing infection within the human body. Thus, the NS3 protease enzyme can be a crucial therapeutic target to be considered in the current study to develop lantadene-based antiviral agents targeting DENV.

The three-dimensional structural model of the NS3 protease enzyme was selected from the PDB database based on the minimum resolution of X-ray used for determination of their structural model, as the lowest resolution of X-ray used in X-ray crystallography results in a more refined structural model of the protein. The procured structure model is then explored to identify the binding cavity in the macromolecular structure by using the DoGSiteScorer module of Protein Plus webserver, which observes the conformational surface of the protein for the presence of cavity or furrow-like structure suitable for strong binding of ligand by using Gaussian filters. Later, the macromolecular structure is prepared for docking by the addition of polar hydrogens and equal distribution of Gasteiger charge. Later, the energy-minimized ligand library was computationally screened against the concerned antiviral target to shortlist the potential leads

having strong binding affinity for the viral drug target and compared with the reference inhibitor 1,8-dihydroxy-4,5-dinitroanthraquinone. The shortlisted leads for the viral NS3 protease enzyme were further screened for their pharmacokinetic profiling based on their physicochemical characteristics, as the considered physicochemical properties govern the rate-limiting steps of absorption, distribution, metabolism, and excretion, which regulates the bioavailability of the proposed molecule at the target site. Compound **62** was proposed as a lantadene-based optimized lead molecule having good binding affinity as well as an optimized pharmacokinetic profile to proceed for MD simulation of 100 ns using the Desmond tool by Schrodinger for evaluating its thermodynamic stability within the binding cavity of the viral NS3 protease enzyme.

Later, the lantadene was isolated from the *L. camara* plant and was further utilized for the chemical synthesis of the desired lantadene analogue, i.e., compound **62**. The synthesized compound **62** was characterized by using diverse spectroscopic techniques and further evaluated for their therapeutic potential against DENV by using *in vitro* cell line-based inhibition assay using A549 cell lines at two different concentrations of 10 or 5 µM and it shows 60 and 45% reduction in DENV titers, respectively.

5 Conclusions

The 78 pentacyclic triterpenoids (Lantadenes) from weed *Lantana camara* L. and their semi-synthetic congeners were virtually screened to predict the potent inhibitors of DENV NS2B-NS3 protease with an *in vitro* assay of lead molecules. In the *in silico* analysis of 78 triterpenoids, two lead molecules (−10.60 and −9.93 kcal/mol) were found to be a viral protease antagonist when compared with the reference ligand 1,8-dihydroxy-4,5-dinitroanthraquinone (−5.377 kcal/mol). At the same time, the lead molecules were studied for binding affinity, pharmacokinetic, and toxicity profiling, along with molecular dynamics simulations. The *in vitro* viral infection inhibition assay indicated that lead molecule **62** leads to a 60 and 45% reduction in DENV titers at 10 and 5 µM concentrations, respectively. The lead molecule **62** can further be optimized for its pharmacophore, and based on the *in silico* and *in vitro* observation for molecule **62**, we are planning for the *in vivo* preclinical studies to confirm the therapeutic efficiency of molecule **62** against DENV followed by clinical trials based on the observed preclinical manifestations.

Funding information: The authors extend their appreciation to the Deputyship for Research & Innovation, Ministry of Education in Saudi Arabia for funding this research through the project number IFP-IMSIU-2023097. The authors also appreciate the Deanship of Scientific Research at Imam Mohammad Ibn Saud Islamic University (IMSIU) for supporting and supervising this project.

Author contributions: Somdutt Mujwar: conceptualization, methodology, investigation, writing – original draft preparation. Jyoti Pal: methodology, visualization. Manu Sharma: methodology, supervision. Abhishek Tiwari: methodology, validation. Varsha Tiwari: validation. Manish Kumar: validation, writing – review and editing, supervision. Shivani Verma: validation, formal analysis, writing – review and editing. Ashraf Ahmed Qurtam: writing – review and editing. Fahd A. Nasr: writing – review and editing. Mohammed Al-Zharani: methodology, writing – review and editing, funding acquisition. Abdulsalam Alhalmi: formal analysis, writing – review and editing.

Conflict of interest: The authors declare no conflict of interest.

Ethical approval: The conducted research is not related to either human or animal use.

Data availability statement: The datasets generated during and/or analyzed during the current study are available from the corresponding author on reasonable request.

References

[1] Lim SP. Dengue drug discovery: Progress, challenges and outlook. Antivir Res. 2019 Mar;163:156–78.
[2] Kumar S, Bajrai LH, Faizo AA, Khateb AM, Alkhaldy AA, Rana R, et al.Pharmacophore-model-based drug repurposing for the identification of the potential inhibitors targeting the allosteric site in dengue virus NS5 RNA-dependent RNA polymerase. Viruses. 2022 Aug;14(8):14081827.
[3] Chitranshi N, Gupta S, Tripathi PK, Seth PK. New molecular scaffolds for the design of Alzheimer's acetylcholinesterase inhibitors identified using ligand- and receptor-based virtual screening. Med Chem Res. 2013;22(5):2328–45.
[4] Kumar SS, Tailor N, Lee HB, Sharma M. Reduced lantadenes A and B: semi-synthetic synthesis, selective cytotoxicity, apoptosis induction and inhibition of NO, TNF-α production in HL-60 cells. Med Chem Res. 2013;22(7):3379–88.
[5] Tailor NK, Jaiswal V, Lan SS, Lee HB, Sharma M. Synthesis, selective cancer cytotoxicity and mechanistic studies of novel analogs of lantadenes. Anticancer Agents Med Chem. 2013 Jul;13(6):957–66.
[6] Tailor NK, Boon HL, Sharma M. Synthesis and in vitro anticancer studies of novel C-2 arylidene congeners of lantadenes. Eur J Med Chem. 2013 Jun;64:285–91.

[7] Suthar SK, Lee HB, Sharma M. The synthesis of non-steroidal anti-inflammatory drug (NSAID)–lantadene prodrugs as novel lung adenocarcinoma inhibitors via the inhibition of cyclooxygenase-2 (COX-2){,} cyclin D1 and TNF-α-induced NF-κB activation. RSC Adv. 2014;4(37):19283–93. doi: 10.1039/C4RA00280F.
[8] Suthar SK, Sharma N, Lee HB, Nongalleima K, Sharma M. Novel dual inhibitors of nuclear factor-kappa B (NF-κB) and cyclooxygenase- 2 (COX-2): synthesis, in vitro anticancer activity and stability studies of lantadene-non steroidal anti-inflammatory drug (NSAID) conjugates. Curr Top Med Chem. 2014;14(8):991–1004.
[9] Monika Sharma A, Suthar SK, Aggarwal V, Lee HB, Sharma M. Synthesis of lantadene analogs with marked in vitro inhibition of lung adenocarcinoma and TNF-α induced nuclear factor-kappa B (NF-κB) activation. Bioorg Med Chem Lett. 2014 Aug;24(16):3814–8.
[10] Sharma M, Sharma PD, Bansal MP, Singh J. Lantadene A-induced apoptosis in human leukemia HL-60 cells. Indian J Pharmacol. 2007;39(3):140–4.
[11] Sharma M, Sharma PD, Bansal MP, Singh J. Synthesis, cytotoxicity, and antitumor activity of lantadene-A congeners. Chem Biodivers. 2007 May;4(5):932–9.
[12] Sharma M, Dev Sharma P, Pal Bansal M, Singh J. Synthesis and antitumor activity of novel pentacyclic triterpenoid lantadene D. Lett Drug Des Discovery. 2007;4:201–6.
[13] Cousins KR. Computer review of ChemDraw Ultra 12.0. J Am Chem Soc. 2011 Jun;133(21):8388.
[14] Berman HM, Battistuz T, Bhat TN, Bluhm WF, Bourne PE, Burkhardt K, et al. The protein data bank. Acta Crystallogr D Biol Crystallogr. 2002 Jun;58(Pt 6 No 1):899–907.
[15] Mujwar S, Pardasani KR. Prediction of riboswitch as a potential drug target and design of its optimal inhibitors for Mycobacterium tuberculosis. Int J Comput Biol Drug Des. 2015 Jan;8(4):326–47.
[16] Mujwar S, Shah K, Gupta JK, Gour A. Docking based screening of curcumin derivatives: a novel approach in the inhibition of tubercular DHFR. Int J Comput Biol Drug Des. 2021 Jan;14(4):297–314. https://www.inderscienceonline.com/doi/abs/10.1504/IJCBDD.2021.118830.
[17] Rani I, Goyal A, Sharma M. Computational design of phosphatidylinositol 3-kinase inhibitors. Assay Drug Dev Technol. 2022 Oct;20(7):317–37.
[18] Pettersen EF, Goddard TD, Huang CC, Couch GS, Greenblatt DM, Meng EC, et al.UCSF Chimera-A visualization system for exploratory research and analysis. J Comput Chem. 2004 Oct;25(13):1605–12.
[19] Rani I, Goyal A. Role of GSK3 (glycogen synthase kinase 3) as tumor promoter and tumor suppressor - A review. Plant Arch. 2019;19:1360–5.
[20] Kaur A, Mujwar S, Adlakha N. In-silico analysis of riboswitch of Nocardia farcinica for design of its inhibitors and pharmacophores. Int J Comput Biol Drug Des. 2016 Jan;9(3):261–76.
[21] Sharma KK, Singh B, Mujwar S, Bisen PS. Molecular docking based analysis to elucidate the DNA topoisomerase IIβ as the potential target for the ganoderic acid; a natural therapeutic agent in cancer therapy. Curr Comput Aided Drug Des. 2020;16(2):176–89.
[22] Minaz N, Razdan R, Hammock BD, Mujwar S, Goswami SK. Impact of diabetes on male sexual function in streptozotocin-induced diabetic rats: Protective role of soluble epoxide hydrolase inhibitor. Biomed Pharmacother. 2019 Jul;115:108897.
[23] Mujwar S, Kumar V. Computational drug repurposing approach to identify potential fatty acid-binding protein-4 Inhibitors to develop novel antiobesity therapy. Assay Drug Dev Technol. 2020 Oct;18(7):318–27.
[24] Jain R, Mujwar S. Repurposing metocurine as main protease inhibitor to develop novel antiviral therapy for COVID-19. Struct Chem. 2020;31(6):2487–99.
[25] Shah K, Mujwar S. Delineation of a novel non-steroidal anti-inflammatory drugs derivative using molecular docking and pharmacological assessment. Indian J Pharm Sci. 2022;84(3):642–53.
[26] Mujwar S, Tripathi A. Repurposing benzbromarone as antifolate to develop novel antifungal therapy for Candida albicans. J Mol Model. 2022 Jun;28(7):193.
[27] Mujwar S, Harwansh RK. In silico bioprospecting of taraxerol as a main protease inhibitor of SARS-CoV-2 to develop therapy against COVID-19. Struct Chem. 2022;33(5):1517–28.
[28] Mujwar S, Pardasani KR. Prediction of riboswitch as a potential drug target for infectious diseases: An insilico case study of anthrax. J Med Imaging Heal Inform. 2015;5(1):7–16.
[29] Behl T, Kumar K, Brisc C, Rus M, Nistor-Cseppento DC, Bustea C, et al. Exploring the multifocal role of phytochemicals as immunomodulators. Biomed Pharmacother. 2021 Jan;133:110959.
[30] Mujwar S, Sun L, Fidan O. In silico evaluation of food-derived carotenoids against SARS-CoV-2 drug targets: Crocin is a promising dietary supplement candidate for COVID-19. J Food Biochem. 2022;46(9):e14219. doi: 10.1111/jfbc.14219.
[31] Fidan O, Mujwar S, Kciuk M. Discovery of adapalene and dihydrotachysterol as antiviral agents for the Omicron variant of SARS-CoV-2 through computational drug repurposing. Mol Divers. 2023 Feb;27(1):463–75.
[32] Ika M, Sharma A, Aggarwal V, Sharma M, Dhingra N. Lantadenes targeting NF-KB in cancer: Molecular docking and ADMET predictions. Int J Life Sci Pharma Res. 2021;11(2):114–22.
[33] Suthar SK, Hooda A, Sharma A, Bansal S, Monga J, Chauhan M, et al. Isolation optimisation, synthesis, molecular docking and in silico ADMET studies of lantadene a and its derivatives. Nat Prod Res. 2021 Nov;35(21):3939–44.
[34] Mujwar S. Computational bioprospecting of andrographolide derivatives as potent cyclooxygenase-2 inhibitors. Biomed Biotechnol Res J. 2021 Oct;5(4):446–50.
[35] Agrawal N, Upadhyay PK, Mujwar S, Mishra P. Analgesic, anti-inflammatory activity and docking study of 2-(substituted phenyl)-3-(naphthalen-1-yl)thiazolidin-4-ones. J Indian Chem Soc. 2020;97(1):39–46.
[36] Shah K, Mujwar S, Krishna G, Gupta JK. Computational design and biological depiction of novel naproxen derivative. Assay Drug Dev Technol. 2020 Oct;18(7):308–17.
[37] Pradhan P, Soni NK, Chaudhary L, Mujwar S, Pardasani KR. In-silico prediction of riboswitches and design of their potent inhibitors for H1N1, H2N2 and H3N2 strains of influenza virus. Biosci Biotechnol Res Asia. 2015;12(3):2173–86.
[38] Mujwar S, Deshmukh R, Harwansh RK, Gupta JK, Gour A. Drug repurposing approach for developing novel therapy against mupirocin-resistant staphylococcus aureus. Assay Drug Dev Technol. 2019 Oct;17(7):298–309.
[39] Arora A, Behl T, Sehgal A, Singh S, Sharma N, Bhatia S, et al. Unravelling the involvement of gut microbiota in type 2 diabetes mellitus. Life Sci. 2021 May;273:119311.
[40] Gielecińska A, Kciuk M, Mujwar S, Celik I, Kołat D, Kałuzińska-Kołat Ż, et al. Substances of Natural origin in medicine: plants vs. Cancer Cell. 2023;12(7):12070986.
[41] Kareem SM, Al-Kadmy IMS, Kazaal SS, Mohammed Ali AN, Aziz SN, Makharita RR, et al.Detection of gyra and parC mutations and

prevalence of plasmid-mediated quinolone resistance genes in klebsiella pneumoniae. Infect Drug Resist. 2021;14:555–63.
[42] Mujwar S. Computational repurposing of tamibarotene against triple mutant variant of SARS-CoV-2. Comput Biol Med. 2021 Sep;136:104748.
[43] Kciuk M, Mujwar S, Szymanowska A, Marciniak B, Bukowski K, Mojzych M, et al. Preparation of novel pyrazolo[4,3-e]tetrazolo[1,5-b][1,2,4]triazine sulfonamides and their experimental and computational biological studies. Int J Mol Sci. 2022 May;23(11):23115892.
[44] Shinu P, Sharma M, Gupta GL, Mujwar S, Kandeel M, Kumar M, et al. Computational design, synthesis, and pharmacological evaluation of naproxen-guaiacol chimera for gastro-sparing anti-inflammatory response by selective COX_2 inhibition. Molecules. 2022;27(20):27206905.
[45] Kciuk M, Mujwar S, Rani I, Munjal K, Gielecińska A, Kontek R, et al. Computational bioprospecting guggulsterone against ADP ribose phosphatase of SARS-CoV-2. Molecules. 2022 Nov;27(23):27238287.
[46] Medigeshi GR, Kumar R, Dhamija E, Agrawal T, Kar M. N-desmethylclozapine, fluoxetine, and salmeterol inhibit postentry stages of the dengue virus life cycle. Antimicrob Agents Chemother. 2016 Nov;60(11):6709–18.
[47] Tăuţan A-M, Ionescu B, Santarnecchi E. Artificial intelligence in neurodegenerative diseases: A review of available tools with a focus on machine learning techniques. Artif Intell Med. 2021 Jul;117:102081.
[48] Chauhan M, Dhar ZA, Gorki V, Sharma S, Koul A, Bala S, et al. Exploration of anticancer potential of Lantadenes from weed Lantana camara: Synthesis, in silico, in vitro and in vivo studies. Phytochemistry. 2023;206:113525.